Lasers in Surgery and Medicine 21:384–394 (1997)

Laser Ablation as a Function of the Primary Absorber in Dentin

Manfred Ostertag, Dr.rer.nat,[1]* James T. McKinley, Ph.D.,[1] Lou Reinisch, Ph.D.,[2] David M. Harris, Ph.D.,[3] Norman H. Tolk, Ph.D.[1]

[1]Center for Molecular and Atomic Studies at Surfaces, Department of Physics and Astronomy, Vanderbilt University, Nashville, TN 37235
[2]Dept. of Otolaryngology, Vanderbilt University Medical Center, Nashville, TN 37232
[3]University of Illinois at Chicago, Chicago, IL 60612

Background and Objective: **Infrared transmission spectra of dentin reveal a broad absorption band between 6.0 and 7.0 μm composed of absorption peaks of water, collagen and carbonated hydroxyapatite. The nearly constant absorption and the existence of absorption peaks of different tissue components were used to investigate ablation as a function of the primary absorber.**
Study Design/Materials and Methods: **Laser ablation of dentin as a function of fluence was studied in the wavelength range between 6.0 and 7.5 μm using the Vanderbilt Free-Electron Laser (FEL). Depth and volume of the ablation crater were determined with a silicon replica method and subsequent confocal laser topometry. SEM investigations were performed on the irradiated surfaces. For the description of the experimental data an ablation model is developed.**
Results: **At all applied wavelengths we found a linear increase of ablation depth as a function of fluence above a threshold fluence. The lower absorption of dentin at 7.5 μm compared to the absorption at 6.0, 6.5 and 7.0 μm results in a greater ablation threshold. At 6.0, 6.5 and 7.0 μm wavelengths the ablation thresholds are comparable. The experimental data are in good agreement with an ablation model using a mean absorption coefficient of the target material. No thermal cracking is observed after ablation in dentin. The post ablative surface structure at 6.0 and 7.0 μm looks similar whereas at 7.5 μm the surface reveals a greater roughness.**
Conclusion: **The ablation efficiency and threshold depend on the mean absorption but do not depend upon the chemical identity of the primary absorber in dentin. Calculations show that heat conduction during the laser pulse leads to a thermal equalization between the heated microstructures and surrounding tissue resulting in an ablation with little dependence on the primary absorber. Lasers Surg. Med. 21:384–394, 1997.**

Key words: ablation model; electron microscopic examination; Free-Electron Laser; infrared absorption; pulsed infrared laser ablation; silicon replica; wavelength variation.

INTRODUCTION

The contact-free application of laser light on dental hard substances was investigated very early in the history of medical laser application [1]. Research on pulsed IR photoablation in dental hard substances in the wavelength ranges be-

Contract grant sponsors: The Alexander von Humboldt Stiftung (Feodor Lynen Grant for M.O.), and in part by the US Office of Naval Research; Contract grant numbers: N00014-91-C-0109, N00014-91-J-4040, and Subprogram grant number: 12403 S3.

*Correspondence to: Manfred Ostertag / Norman Tolk, Box 1807B Vanderbilt University, Nashville, TN 37235, USA, Phone: (615) 322278, Fax: (615) 3431708

tween 1 and 3 μm and between 9 and 11 μm has been carried out by many groups [2]. Comparisons between such studies are sometimes difficult due to different applied laser parameters i.e., beam profile, fluence and temporal pulse shape. Additionally, ablation experiments were restricted to wavelengths available by commercial laser sources. Measurements using a free-electron laser (FEL) minimize such difficulties due to a wide and continuous tunability of the wavelength while other laser parameters are unchanged and provide additional data at infrared wavelengths not available with solid-state or CO_2 lasers.

In the past several years, a variety of FEL user facilities have been developed to provide scientific researchers with mid- and far-infrared radiation of unparalleled brightness and tunability (a survey of the FELs and their parameters is given in [3]). The experiments described in this paper were performed at the Vanderbilt FEL Center for Biomedical and Materials Research.

Dentin consists of approximately 25% water, 30% organic materials (mainly collagen) and 45% (carbonated) hydroxyapatite (HAP) [4]. According to absorption spectra, the individual components of dentin reveal IR absorption peaks at around 3.0 μm (water, OH in apatite), 6.0 μm (water, amide I - collagen), 6.5 μm (amide II - collagen), 7.0 μm (carbonated hydroxyapatite) and 9.5 μm (phosphate absorption bands of apatite). The absorption bands are listed in Table 1 in greater detail. Generally, IR laser wavelengths exhibit different mean absorption depths in dental hard tissues but also result in different heating efficiencies of the individual components of water, organic materials and HAP. For example, irradiating dentin with a CO_2 laser at 9.6 μm or an Er:YAG laser at 2.9 μm results in heating of HAP or tissue water, respectively, by the direct absorption of laser radiation. Further below we show by theoretical estimations that heat conduction should lead to a thermal equalization between pronounced heated components and surrounding tissue during a laser pulse of the order of few μs. If one assumes a thermal ablation model, then the ablation efficiency and threshold are independent of the (main) primary absorber of laser radiation and a scaling of the results with the mean absorption coefficient of the target material would be expected.

The goal of the this study is to investigate ablation in dentin for various heating efficiencies of the individual components i.e., different (main) primary absorber of radiation inside the tissue. Since the most promising lasers for application in dentistry are solid-state lasers around 3 μm and CO_2 lasers, the influence of the primary absorber on ablation is not only of basic but also of clinical interest.

Absorption spectra of dentin reveal a near constant value of absorption for the peaks at 6.0, 6.5 and 7.0 μm [5], thus allowing one to test the influence of the primary absorber of radiation on ablation while influences due to variation of absorption are minimized. Since the absorption depth of photons in dentin in this wavelength range is around 4 μm (see appendix 2) and the infrared beam at the Vanderbilt FEL is delivered in approximately 5 μs duration macropulses, these factors results in a confinement of heat within a volume according to Lambert-Beers law during one macropulse. With a macropulse energy up to 100 mJ together with a repetition rate up to 30 Hz [6] the Vanderbilt FEL is the appropriate laser for performing ablation experiments in this wavelength range.

Measurements were performed in the range between 6.0 and 7.0 μm due to the small variation of absorption and due to the existence of absorption peaks of water, collagen and carbonated hydroxyapatite. The wavelength 7.5 μm, which exhibits a mean absorption less than the wavelengths between 6.0 and 7.0 μm, was studied for comparison. The experimental data are compared with an ablation model based on Lambert-Beers law and using the mean absorption coefficient of the target material.

MATERIALS AND METHODS

Sample preparation: Nine human wisdom teeth, extracted less than a week before the experiment, were used. The teeth were cut with a diamond saw into planoparallel thin sections of about 1 mm thickness. The obtained sections were smooth but not polished. The extracted teeth as well as the sections were kept in sterile saline and stored at approximately 5°C until 2 hours before the ablation experiment.

Experimental set-up: Measurements were performed with the Vanderbilt Free-Electron Laser (FEL) [6]. The macropulse revealed a linear decrease of pulse length in the investigated wavelength range (5.5 μs at 6.0 μm and 4.3 μs at 7.5 μm)[7]. The macropulse repetition rate was kept

constant at 1 Hz. Each macropulse consisted of a track of micropulses with a pulse duration of about 1 ps at a repetition rate of 2.8 GHz [6]. The beam transport system was supplemented by a planar and a spherical mirror with a focal length of 50 cm. The sample was fixed 2.7 cm behind the focus of the beam. The diameter (FWHM) and the fluence in the center of the Gaussian beam profile F_0 at the sample surface were calculated according to the experimental set-up using equations for Gaussian beam propagation and the FWHM diameter of the Gaussian FEL beam. According to the calculations the FWHM increases from 0.64 mm at 6.0 μm to 0.71 mm at 7.5 μm. To perform at each wavelength a fluence variation without a change of beam profile, the laser radiation was attenuated with germanium neutral density filters (constant transmission between 4.0 and 8.0 μm; transmission values: 0.68, 0.33 and 0.13).

The energy per pulse was monitored on-line by an energy meter (Molectron J4-09, USA) using a fraction of the FEL output, reflected from a planar BaF_2 beamsplitter. To account for losses of radiation due to absorption in air, the distances from the beamsplitter to the energy meter and from the beamsplitter to the sample surface were chosen to be the same length. Prior to the main ablation experiments the energy meter was calibrated against an absolute energy meter (Scientech 365, Power and Energy Meter, USA). For calibration, the absolute energy meter was placed at the same position as the samples.

Ablation experiment: Ablation experiments in dentin were performed at the 6.0, 6.5, 7.0 and 7.5 μm wavelengths. Before a sequence of ten pulses, a surplus of saline was carefully removed from the exposed surface using dry lens paper. Ten pulses were applied to each crater. At least five arbitrary sections of the total of twelve sections were used for each wavelength. During the whole experiment the exposure time of the wet samples to air was less than 2 minutes. After the experiment the sections were stored in saline at 5°C for further analysis.

Measurement and evaluation of crater profile, SEM observations: The ablation craters obtained were examined by means of a silicon replica method and subsequent confocal laser topometry (UBM Microfocus Messystem, UBM, Ettlingen, Germany) as described previously [8]. Prior to the replication process the sections were rinsed in de-ionized water and air-dried. The resultant digitized data of the measured crater profile were evaluated for ablation depth as well as for the volume of the ablation crater. Irradiated areas where no negative crater profile was found on the silicon replica the ablation depth as well as the volume was set equal to zero. Random sections were rinsed in de-ionized water, dried, attached to aluminum stubs and sputtered with a 10 - 12 nm thick layer of gold. They were then examined in a Cambridge S250 scanning electron microscope (SEM) at 15 kV.

RESULTS

Examples of the ablation crater profile are displayed in Figs. 1 and 2. Fig. 1 shows the 3-d profile and Fig. 2 a line scan of an ablation crater after irradiating dentin with 7.0 μm laser light.

The obtained crater depths as a function of fluence for the 6.0 μm wavelength is shown in Fig 3. Each displayed value is the total depth in the center of the ablation crater after ten laser pulses vs. the average fluence in the center of the Gaussian beam. The error obtained by the evaluation of a digitized crater profile (least square fit by Gauss: fit of a constant function to the measured data at the bottom of the ablation crater) were in the range between 0.5 and 1.5 μm and thus small in comparison to the variation of the total ablation depth due to material related variations of the samples. We were able to measure crater depths as small as 5 - 10 μm, *i.e.*, ablation depth per pulse as small as 0.5 - 1.0 μm.

Additional linear regressions are shown in Fig. 3 (Gaussian least square fit of a linear function to the experimental values excluding values with zero ablation depth). The intersection of the linear regression with the fluence axis gives the ablation threshold F_v. The ablation thresholds as well as the slopes (dx/dF) of the linear regressions are listed in Table II.

The ablation threshold is lower for the 6.0, 6.5 and 7.0 μm wavelengths compared to the 7.5 μm wavelength. Within experimental uncertainty the slope of the linear regression is the same for the wavelengths 6.0, 6.5 and 7.5 μm whereas the slope is reduced for the 7.0 μm wavelength.

The measured ablated volume as a function of the measured ablation depth is displayed for each ablation crater for 6.0 and 7.0 μm wavelengths in Fig. 4. No significant difference of ablated volume as a function of ablation depth is observed between these wavelengths.

SEM photos of dentin after irradiation with

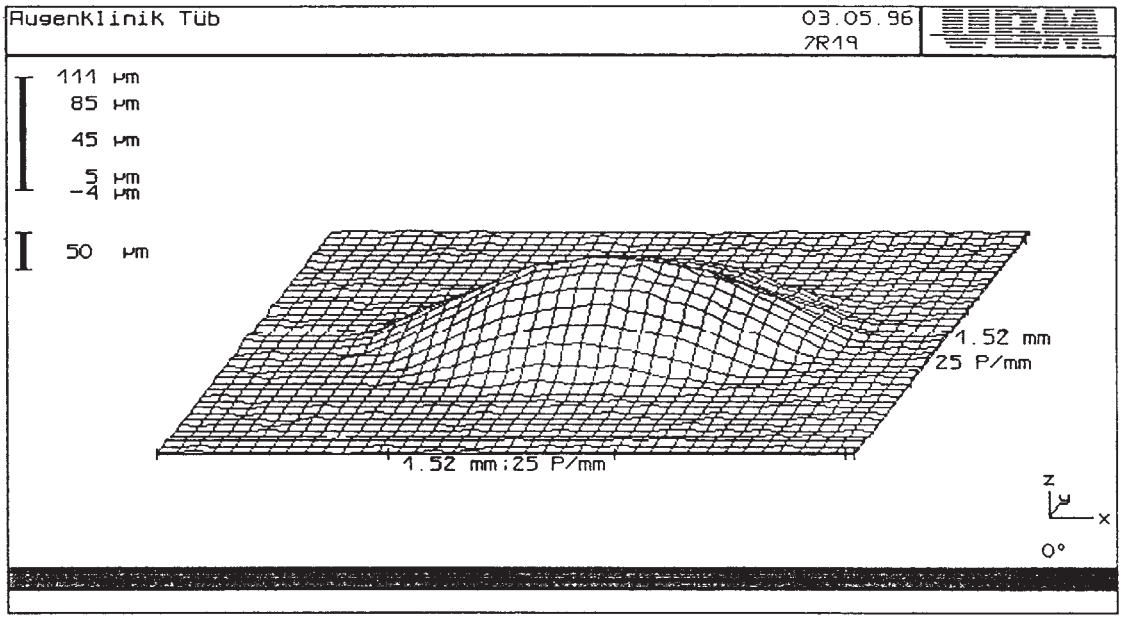

Fig. 1: The negative ablation crater profile measured on the silicone replica using a confocal laser topometer (target material: dentin, wavelength: 7.0 µm, energy per pulse: 27.1 mJ, fluence per pulse: 5.1 J/cm^2, ten applied laser pulses).

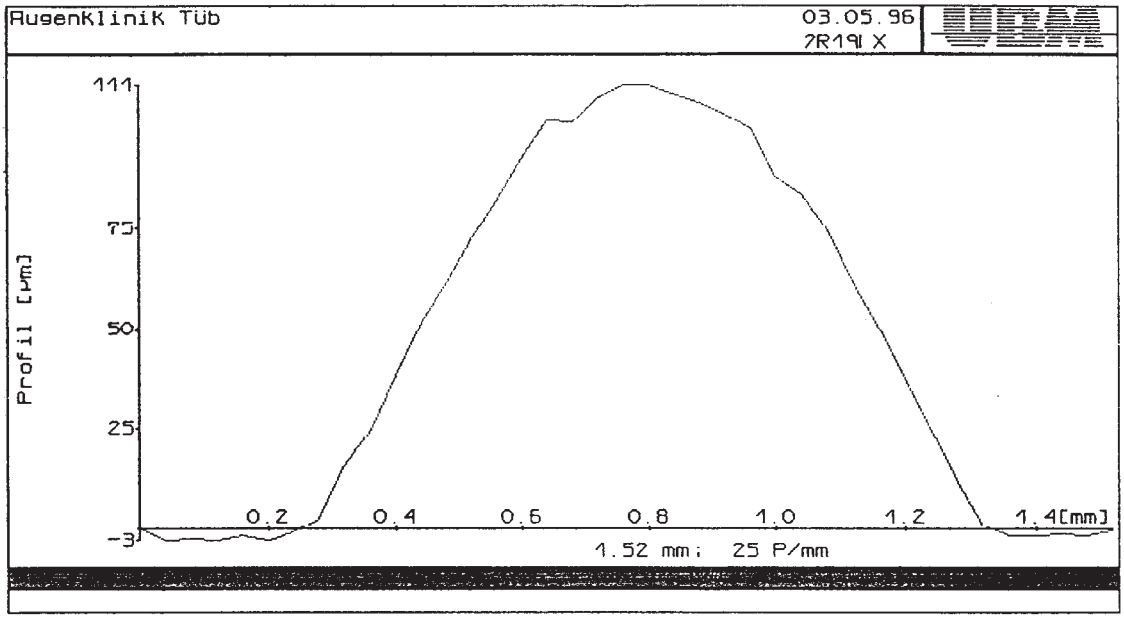

Fig. 2: A line scan through the center of the negative ablation crater of fig 1. is shown. The profile reflects our Gaussian beam profile.

laser light at the 6.0, 7.0 and 7.5 µm wavelengths are presented in Figs. 5 a, b and c, respectively. The photos show the surface area in the center of the ablation crater. In none of the photos is there evidence of molten and rehardened dentin. After irradiation with laser light at the 6.0 and 7.0 µm wavelength the surface structure looks similar. In contrast, at 7.5 µm wavelength the surface seems to reveal increased roughness.

DISCUSSION

Theoretical Model for Photoablation: A model based on Lambert-Beers law was chosen to

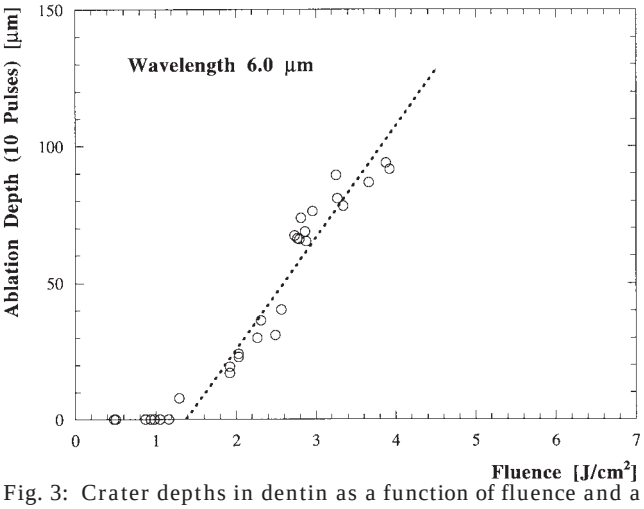

Fig. 3: Crater depths in dentin as a function of fluence and a linear regression of the experimental data are shown (applied laser wavelengths: 6.0 μm; ten pulses applied per crater).

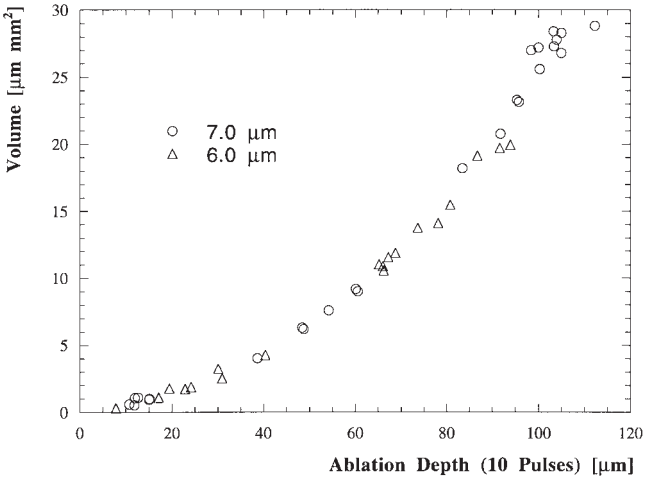

Fig. 4: Crater volumes *i.e.*, ablated volumes as a function of the measured ablation depths are displayed for each ablation crater for the 6.0 and 7.0 μm wavelengths.

TABLE 1 Absorption Bands for Various Absorbers in Dentin

Group	Absorption frequency (cm^{-1})	Absorption wavelength (μm)
Carboxyl (mineral)	1,460	6.8
	1,414	7.1
	1,156	8.65
	1,138	8.8
Amide (protein)	1,684	5.94
	1,641	6.1
	1,595	6.3
	1,461	6.8
Phosphate (mineral)	1,030	9.7
Hydroxyl (water & protein)	3,400	2.9
	1,630	6.1

describe the experimental data (ablation depth per pulse). In this model, we ignore any acoustic effects on the ablation rate. Models of the acoustic shock-wave generation show that the micropulse structure from the FEL does not construct a train of shock waves. Instead, one shock wave is generated from the macropulse structure of the FEL.[9] The model calculation also correlates with measured shockwaves as a function of absorption coefficient and FEL macropulse length.

We implicitly assume the tissue has time independent absorption. The irradiance I_0 at the surface is assumed to be constant over the ablation area A and during the pulse duration t (these assumptions are made only for transparency of the calculations and are not necessary, as is indicated in appendix 1). With E the pulse energy, $F = E/A$ the fluence and α the mean absorption coefficient of the material are denoted. According to Lambert-Beers law, the irradiance $I(x)$ in the depth x of the material is given by

$$I(x) = I_0 \exp(-\alpha x) \text{ with } I_0 = F/\tau \qquad (1)$$

After the start of the laser pulse, the temperature or in other words - the energy density within the material, increases due to the absorption of light. Ablation of material will start when a critical temperature or energy density is obtained. For the calculations, we assume in the following that heat conduction to material outside the irradiated volume during the pulse (time scale μs) can be neglected and that heat deposited within the material during a single laser pulse completely dissipates before the arrival of the next pulse (time scale ms - see appendix 2). Thus each pulse starts with the same initial temperature of the material. Before ablation starts, with equation (1) the energy density $e(x,t)$ in the material at the depth x and the time t ($t = 0$ at the start of the pulse) is described as follows

$$e(x,t) = \int_0^t -\frac{dI(x)}{dx}\, dt' = I_0 \alpha t \exp(-\alpha x) \qquad (2)$$

We denote the critical energy density for ablation with e_v and the time between the beginning of the pulse and the start of ablation with t_v . The product $e_v \Delta V$ can be interpreted as the energy needed to remove a volume element ΔV. With equation (2) one obtains for t_v

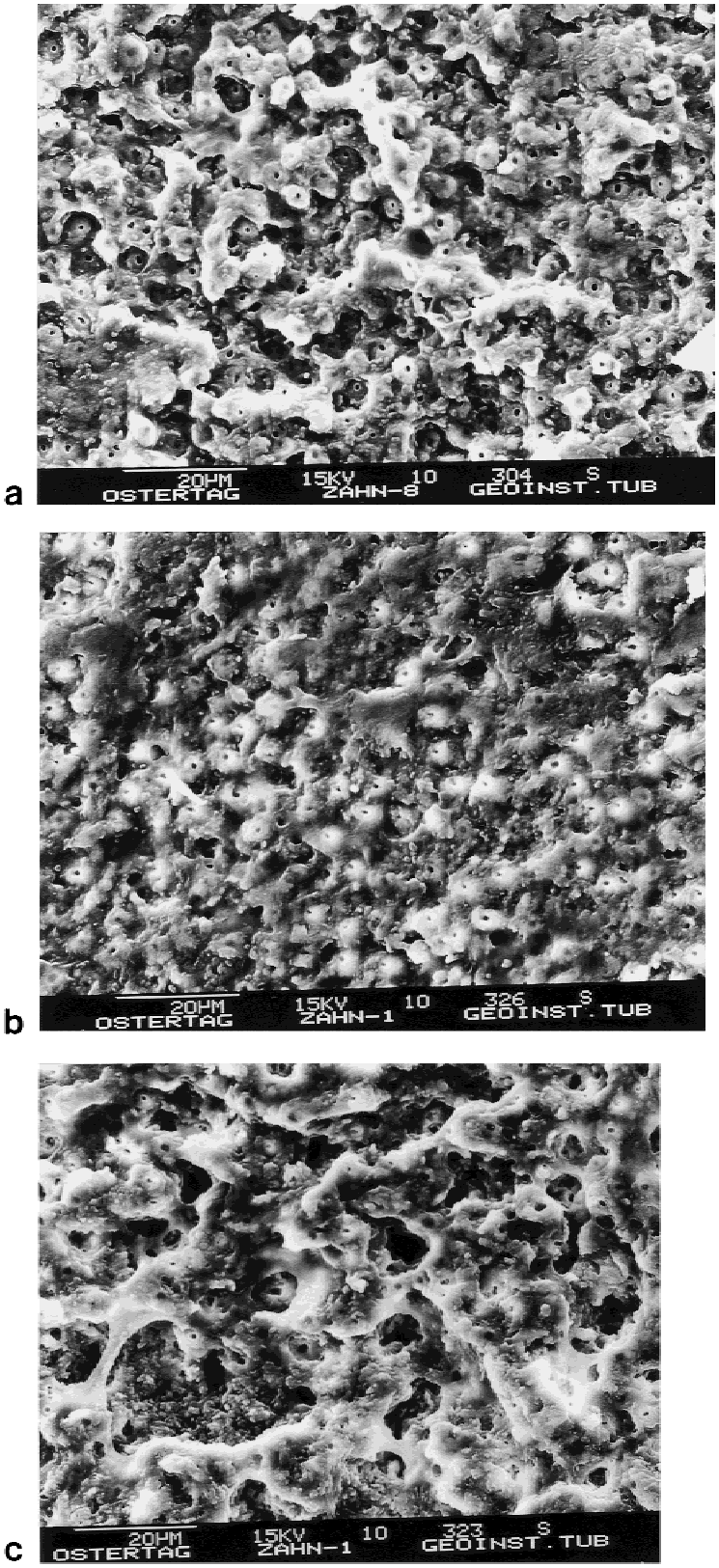

Fig. 5: Scanning Electron Microscope (SEM) photographs after ablation of dentin with the laser wavelengths 6.0 **(a)**, 7.0 **(b)**, and 7.5 µm **(c)**. All photographs show the center of an ablation crater, the magnifications are given in the photographs (fluence: 2.86 J/cm^2 (a), 5.00 J/cm^2 (b), 5.46 J/cm^2; energy per pulse 13.1 mJ (a), 26.6 mJ (b), 31.2 mJ (c)).

$$t_v = \frac{e_v}{I_0 \alpha} \tag{3}$$

Clearly, ablation occurs only for a pulse length $\tau > t_v$ (or with equations (1) and (2) $F > e_v/a$). At the time t_v, one needs for the ablation of an infinitesimal layer of thickness Δx, an additional increase of energy density Δe given by

$$\Delta e = -\left.\frac{de(x,t_v)}{dx}\right|_{x=0} \Delta x = e_v \alpha \Delta x \tag{4}$$

According to equation (2) the infinitesimal time Δt needed to obtain the additional energy density Δe is given by

$$\Delta e = -\left.\frac{dI(x)}{dx}\right|_{x=0} \Delta t = I_0 \alpha \Delta t \tag{5}$$

With the help of equations (4) and (5) the ablation velocity v at the beginning of the ablation process is given by

$$v = \frac{\Delta x}{\Delta t} = \frac{I_0}{e_v} \tag{6}$$

It is demonstrated in appendix 1 that for times $t_v < t < \tau$ and a rectangular temporal pulse shape, the ablation velocity is given by equation (6) and thus independent of time. The ablation velocity depends only upon the irradiance I_0 and the critical energy density e_v. The fact that the ablation velocity is independent of the absorption coefficient and dependent upon the irradiance has been verified by cw laser experiments [10]. The ablation depth per pulse x_p is finally given by equations (1),(3), and (6)

$$x_p = v(\tau - t_v) = \frac{1}{\alpha}\left(\frac{F}{F_v} - 1\right) \tag{7}$$

with $F_v = e_v/\alpha$. For the case $F < F_v$ no ablation occurs. Thus F_v can be interpreted as the threshold fluence for ablation. Due to the assumption that heat conduction out of the irradiated volume during the laser pulse is negligible, the result in equation (7) is independent of the temporal shape and duration of the pulse (see appendix 1). For cases with $F \gg F_v$ equation (7) reduces to

$$x_p = \frac{F}{e_v}$$

The irradiance over the ablation was assumed to be constant for the calculations. In practical terms this is not achievable. Equation (7) can be generalized for cases with a variable local irradiance over the ablation area by describing the local irradiance by a two dimensional profile function. The evaluated equation describes the obtained crater profile after the photoablation process (see appendix 1).

For the evaluation of the experimental data an equation independent of the applied fluence is deduced using equation (7).

$$\frac{dx_p}{dF} F_v = \frac{1}{\alpha} \tag{8}$$

Discussion of Results

The measured ablation depth in dentin plotted versus mean fluence per laser pulse reflects a linear relationship for all applied laser wavelengths (and $x_p > 0$). The intersection of the linear regression with the fluence axis gives the ablation threshold F_v . The ablation thresholds as well as the slopes of the linear regressions are given in Table II.

Since the depths of the craters are less than their FWHM, vignetting effects during ablation are negligible.

Estimations of the absorption depths $1/a$ in dentin using equation (8) were performed and are listed in Table II. In accordance with the theoretical model, a larger absorption coefficient *i.e.*, a smaller absorption depth of the photons in the target material, leads to a lower ablation threshold F_v and thereby to an increasing crater depth x_p (see Table II and equation (7)). Also, according to our theorectical model, a high ablation depth *i.e.*, ablation volume per pulse, is obtained when less (thermal) energy is left in the target material after ablation [8]. Thermal energy left inside the target material after ablation is one reason for resultant collateral thermal damage.

In contrast to the linear relationship of ablation depth vs. fluence found in our experiments other groups found that a logarithmic relationship result in a better description of the ablation in dentin (for example Hibst et al. [11] and Li et al. [12]; Er:YAG laser, 2.94 μm, pulse length 250 μs). However, these groups used much longer pulses and the assumption of thermal confinement is probably not valid for their experimental conditions. Forrer et al. [13] measured the ab-

TABLE 2. Slopes (dx_p/dF), Ablation Thresholds (F_v) and the Products [$(dx_p/dF)F_v$] of the Experimental Ablation Depth per Pulse in Dentin as a Function of Fluence Given for 6.0, 6.5, 7.0, and 7.5 μm Wavelengths*

Wavelength (μm)	6.0	6.5	7.0	7.5
dx_p/dF (μm cm^2/J)	3.93 ± 0.29	3.95 ± 0.27	2.75 ± 0.06	3.98 ± 0.19
F_v(J/cm^2)	1.30 ± 0.11	1.61 ± 0.07	1.23 ± 0.06	2.76 ± 0.11
$(dx_p/dF)F_v$ (μm)	5.11 ± 0.57	6.36 ± 0.52	3.38 ± 0.18	10.98 ± 0.68
Dentin (lower limit)1/α (μm)	1.6	2.3	1.8	6.7
Dentin (upper limit) 1/α (μm)	6.2	61.7	9.5	73.2

*Additional estimations of the mean free path of photons in dentin (appendix 2 - dentin (lower limit); dentin (upper limit)) are displayed.

sorption of the laser radiation in the ablation plume during ablation in bone with a CO_2 laser (pulse length 150 μs). They found that the relative absorption of radiation in the ablation plume increases with an increasing fluence (0 - 10% for 2.5 - 5 J/cm^2, 10 - 30% for 40 J/cm^2 and 30 - 60% for 370 J/cm^2). Bone and dentin consist of the same components with approximately the same relative amounts. Hibst et al. examined crater depth versus fluence for higher fluences (only one value with a fluence smaller than 10 J/cm^2). The logarithmic relationship found by Hibst et al. and Li et al. might also be a result of laser radiation absorption and scattering in the ablation plume. In contrast, the absorption and scattering of radiation in the ablation plume during our experimental investigations is less due to the lower applied fluence (F_0 < 7 J/cm^2).

The diameter of hydroxyapatite crystals is on the order of 100 nm and is thus approximately 40 times less than the absorption depth of photons [8]. An estimation showed [8] that the time for thermal relaxation of a heated crystal is approximately 100 times less than the duration of the laser light pulse. Thus heat conduction during the laser pulse leads to a thermal equalization between pronounced heated micro structures and surrounding tissue and e_v should be independent of the wavelength.

Other structures in the dentin, such as the tubules and the peritubular dentin are much larger than the hydroxyapatite crystals. The tubules are on the order of microns in diameter. The diameter distances are still within thermal relaxation times of the FEL pulse (approximately 5 μs pulse). The heat does not have to equilibrate along the entire length of the tubule (these can extend on the order of mm). It is only important that the tubules are in thermal equilibrium with the surrounding material in the irradiated volume. In accordance to the estimation the ablation thresholds for wavelengths with approximately the same mean absorption in dentin *i.e.*, at 6.0, 6.5 and 7.0 μm are comparable.

According to the ablation model and the above estimation the increase in ablation depth vs. fluence should be independent of the applied laser wavelength. Within experimental uncertainty the rise is similar for the 6.0, 6.5 and 7.5 μm wavelengths but significantly less for 7.0 μm. The wavelength 7.0 μm seems to be less effective for ablation of dentin compared to the other wavelengths. For the evaluation of equation (7) it was assumed in equation (1) that the irradiance $I(x=0)$ is equal to I_0 or in other words a (wavelength dependent) reflectance of the incident laser light at the air - dentin interface was neglected. Duplain *et al.* [14] measured the complex index of refraction of dental enamel at CO_2 laser wavelengths between 9.2 and 10.7 μm. They found a strong wavelength dependence of the complex index of refraction that corresponds to a well-known absorption band of hydroxyapatite. For example Duplain found from a wavelength of 9.5 to 10.7 μm a decrease of reflectance from 50% to 10% *i.e.*, the highest reflectivity was found at 9.5 μm. Thus the smaller rise of ablation depth versus fluence at 7.0 μm may be a result of an increased sample reflectivity [15].

It has to be noted that a (wavelength dependent) error of the scaling factor between energy per pulse and fluence in the center of the Gaussian beam as well as a (wavelength dependent) reflectivity at the air - dentin interface does not affect the result of absorption depth obtained in equation (8). Yet, temporarily and permanent changes of reflectivity as a function of fluence due to phase changes of complex minerals during strong heating as found by Fried et al. [16] can affect the result of the obtained absorption depth. However, our data do not indicate that these are significant changes that we must take into account.

Time-resolved measurements of the macro-

pulse as a function of wavelength revealed in the investigated wavelength range a linear decrease of pulse length (5.5 μs at 6.0 μm - 4.3 μs at 7.5 μm) [7]. The thermal relaxation time of a heated volume according to Lambert-Beer's law is approximately a factor of 20 greater than the pulse length (see appendix 2). Thus we assume the change of macropulse length as a function of wavelength had only minor affects on the experimental results. In a previous paper it was shown that the FEL's macropulse, composed of ps micropulses at high repetition rates (GHz region), has no major influence on the ablation rate or the pattern of collateral thermal damage [8].

Radial cracks are not observable for any wavelength after our ablation experiments. One might observe radial cracks and concentric fissures from rapid heating and cooling of the dentin. Photoacoustic stress waves could also cause cracking in the dentin. None of these is observed.

Thermal damage of such a kind occurs if heat conduction into the surrounding tissue plays a significant role during the whole ablation procedure. Using a pulse length of about 5 μs and an absorption depth of photons between 4 and 12 μm a confinement of heat inside the volume according to Lambert-Beer's law is obtained during the laser pulse. Between subsequent macropulses heat conduction results in a distribution of the energy left in the tissue after a laser pulse. Due to the confinement of heat during a laser pulse and the low absorption depth of photons the total energy left in the tissue is small and results in a negligible pile-up of heat during a sequence of ten pulses. This is consistent with our observations.

This model has neglected photoacoustic contributions to the ablation process. The model is obviously an oversimplification of the actual system. However, we note that this simplistic model appears to be sufficient to describe the data. As such, these data do not warrant a more complicated model.

The photoacoustic stress transients would depend upon the laser intensity, the absorption coefficient of the dentin, and the macropulse duration for the conditions of these experiments.[9] Given the near constant absorption coefficient and the near constant laser pulse length, ablation processes due to the photoacoustic stress transients would scale with laser intensity similar to the thermal ablation model given above. Thus, the idea of thermal equalization appears to be valid and independent of the ablation mechanism for these experiments.

In conclusion: A thermal equalization between pronounced heated microstructures and the surrounding tissue leads to an ablation that is largely independent of the primary absorber. The results are in good agreement with the developed ablation model that uses the mean absorption coefficient of the target material.

Appendix 1

We take in the following - in contrast to equation (1) - a time and space dependent irradiance into account. The local irradiance is given by

$$I(r,\phi.x,t) = F(r,\phi)\, f(t)\exp(-\alpha x) \qquad (9)$$

with $\int_0^\tau f(t)dt = 1$ and $\int F(r,\phi) r dr d\phi = E$

where $F(r,\phi)$ describes the space dependent fluence and $f(t)$ the temporal pulse profile. Neglecting heat conduction during the pulse length, one obtains for the energy density before ablation starts

$$e(r,\phi,x,t) = \int_0^t F(r,\phi) f(t')\alpha\exp(-\alpha x)dt' \qquad (10)$$

The equation above disregards the scattering of photons in the target material. But even when scattering of photons takes place in the target material, equation (10) is valid for cases in which the value of the local irradiance does not vary much over a distance equal to the absorption depth $1/\alpha$ of the photons. In our experiment $1/\alpha$ is less than 20 μm and the FWHM of our Gaussian beam greater than 0.5 mm and thus equation (10) can be used.

Ablations occurs for places with

$$\int_0^t F(r,\phi)\alpha f(t')dt' = F(r,\phi)\alpha > e_v$$

The time $t_v(r,\phi)$ between the beginning of the pulse and the start of ablation at a place (r,ϕ) is given by

$$\int_0^{tv(r,\phi)} F(r,\phi)\alpha f(t')dt' = e_v \qquad (11)$$

The position of the moving material surface at the place (r,ϕ) is denoted with $x_0(r,\phi,t)$. A moving coordinate system is used for the calculation of the energy density within the material with $z(r,\phi,t) =$

($x - x_0(r,\phi,t)$. For the moving coordinate system one obtains instead of equation (5)

$$F(r,\phi)f(t)\alpha \exp(-\alpha z) = -\frac{\partial e(r,\phi,z,t)}{\partial z}\frac{\partial x_0(r,\phi,t)}{\partial t} + \frac{\partial e(r,\phi,z,t)}{\partial t} \quad (12)$$

$$v(r,\phi,t) = \frac{\partial x_0(r,\phi,t)}{\partial t}$$

is the place and time dependent ablation velocity. The solution of equation (12) is given by

$$e(r,\phi,z,t) = e_v \exp(-\alpha z) \text{ and } v(r,\phi,t) = \frac{F(r,\phi)}{e_v} f(t)$$

The ablation depth per pulse at the place (r,ϕ) is finally using equation (10)

$$d(r,\phi) = \int_{tv(r,\phi)}^{\tau} \frac{F(r,\phi)}{e_v} f(t')dt' = \frac{1}{\alpha}\left(\frac{F(r,\phi)}{F_v} - 1\right)$$

with $F_v = e_v/\alpha$. This model results in an ablation depth independent of the temporal pulse shape. For cases with a constant local irradiance at the surface the equation above reduces to equation (7).

Appendix 2

The mean free path of photons and the reflectivity in bovine enamel at the wavelength 10.3 μm is 1.54 μm and 0.156, respectively [16]. Assuming that scattering of photons was negligible in the transmission measurement of [5], assuming the absorption in dentin at 10.3 μm is dominated by absorption of HAP and using the percentage of HAP in enamel (85%) and dentin (45%), the effective thickness d of the dentin sample used in [5] can be calculated. We obtained d = 0.95 ± 0.15 μm. Using coefficients of reflectivity of R = 0.10 and R = 0.35 we obtained a lower and upper limit for the mean free path of photons in dentin for the 6.0, 6.5, 7.0 and 7.5 μm wavelengths. The values are displayed in table II (lower limit: R = 0.1, d = 0.8 μm and upper limit: R = 0.35, d = 1.1 μm). Using at the wavelength 7.5 μm the parameter set for the upper limit gives a less transmission than measured in [5]. Therefore it is not possible to determine an upper limit of absorption depth in dentin by using this parameter set. Since the absorption of water is well known we determined the upper limit in this case by:

(absorption depth in pure water)
* (volume percent of water in dentin).

The relaxation time for a heated volume according to Lambert-Beer's law is less than 50 ms (greater than 10 μs), assuming that the absorption depth of radiation inside the tissue is smaller than 50 μm (greater than 2 μm) [15].

ACKNOWLEDGMENTS

The authors are indebted to John Werther, DMD, MD for providing the fresh teeth samples, and Dr. Benedikt Jean in Germany for use of the Topometer UBM and the SEM in the evaluation of data. Dr. M. Ostertag acknowledges a grant from the Alexander von Humboldt Stiftung. This work was supported in part by the US Office of Naval Research, #N00014-91-C-0109 and #N00014-91-J-4040.

REFERENCES

1. Stern RH, Sognnaes RF. Laser beam effect on dental hard tissues. J Dent Res 1964; 43 (Suppl.):873 (Abs 307).
2. Wigdor HA, Walsh JT, Featherstone JDB, Visuri SR, Fried D, Waldvogel JL. Lasers Surg Med 1995; 16:103-133.
3. Tolk NH, McKinley JT, Margaritondo G. Surf Rev and Lett 1995; 2:501-512.
4. Seekamp C, Lösche G, Ertl T, Scholz C. Theorie und Praxis der Laseranwendung in der Zahn- Mund- und Kieferheilkunde VI - 3.3.1, 3.2 Dentinkonditionierung. In: Berlien HP, Mueller G, eds. Angewandte Lasermedizin. Landsberg/Lech: ecomed, verlagsgesellschaft 1993: 51-62.
5. Dörschel K, Ertl T, Mueller G. Theorie und Praxis der Laseranwendung in der Zahn-, Mund- und Kieferheilkunde VI - 3.3.1, 2.1 Physikalische Grundlagen des Lasereinsatzes in der Zahnheilkunde. In: Berlien HP, Mueller G, eds. Angewandte Lasermedizin. Landsberg/Lech: ecomed, verlagsgesellschaft 1993:5-11.
6. Brau CA. The Vanderbilt University free-electron laser center. Nucl Instrum Meth 1992; A3 19:47-50.
7. Harris DM, Reinisch L, Edwards G, Yessik M, Ashrafi S, Santos-Sacchi J. Mid-infrared ablation of dentin with the Vanderbilt FEL. SPIE Proceedings 1996; 2672:165-175.
8. Ostertag M, Walker R, Koster KU, Hüttemann H, Geis-Gerstorfer J, Weber H, Tolk N, Jean B. Photoablation around the Absorption Peak of Hydroxyapatite. J Dent Res (in press).
9. Lamb DC, Doukas A, Flotte T, Reinisch L, Ossoff RH, Therapeutic Applications of Laser-Induced Pressure Waves. Laser Surg Med 1995:**7,** 73.
10. Gijsbers GHM, Selten FM, van Gemert MJC. CW Laser Ablation Velocities as a Function of Absorption in an Ex-

perimental One-Dimensional Tissue Model. Lasers Surg Med 1991; 11:287- 296.
11. Hibst R, Keller U. Experimental Studies of the Application of the ER:YAG Laser on Dental Hard Substances: I. Measurement of the Ablation Rate. Lasers Surg Med 1989; 9:338-344.
12. Li Z, Code JE, van de Merwe WP. Er:YAG Laser Ablation of Enamel and Dentin of Human Teeth: Determination of Ablation Rates at Various Fluences and Pulse Repetition Rates. Lasers Surg Med 1992; 12:625-630.
13. Forrer M, Frenz M, Romano V, Altermatt HJ, Weber HP, Silenok A, Istomyn M, Konov VI. Bone-Ablation Mechanism Using CO_2 Lasers of Different Pulse Duration and Wavelength. Appl Phys B 1993; 56:104- 112.
14. Duplain G, Boulay, Belanger PA. Complex index of refraction of dental enamel at CO_2 laser wavelengths. Appl Opt (1987); 26:4447-4451.
15. Ostertag M, Walker R, Weber H, vd Meer L, McKinley J, Tolk N, Jean B. Ablation in Teeth with the Free-Electron Laser around the Absorption Peak of Hydroxyapatite (9.5 μm) and between 6.0 and 7.5 μm. SPIE Proceedings 1996; 2672:181-192.
16. Fried D, Glena RE, Featherstone JDB, Seka W. Permanent and Transient Changes in the Reflectance of CO_2 Laser Irradiated Dental Hard Tissues at $\lambda = 9.3$, 9.6, 10.3, and 10.6 μm and at Fluences of l-20 J/cm2. Lasers Surg Med 1996 (in press).